Langmuir Article

pubs.acs.org/Langmuir

On the Thermal Conductivity of Gold Nanoparticle Colloids

Natallia Shalkevich,[†] Werner Escher,[‡,§] Thomas Bürgi,*[,†,⊥] Bruno Michel,[§] Lynda Si-Ahmed,[∥] and Dimos Poulikakos[‡]

[†]*Université de Neuchâtel, Institut de Physique, Laboratoire de chimie physique des surfaces, Rue Emile-Argand 11, 2009- Neuchâtel, Switzerland,* [‡]*Laboratory of Thermodynamics in Emerging Technologies, Department of Mechanical and Process Engineering, ETH Zurich, 8092 Zurich, Switzerland,* [§]*IBM Research GmbH, Zurich Research Laboratory, 8803 Rüschlikon, Switzerland,* [⊥]*Ruprecht-Karls-Universität Heidelberg, Physikalisch-Chemisches Institut, Im Neuenheimer Feld 253, 69120 Heidelberg, Germany, and* [∥]*Metalor Technologies SA, Av. du Vignoble, Case postale 9, 2009 Neuchâtel 9, Switzerland*

Received June 24, 2009. Revised Manuscript Received July 20, 2009

Nanofluids (colloidal suspensions of nanoparticles) have been reported to display significantly enhanced thermal conductivities relative to those of conventional heat transfer fluids, also at low concentrations well below 1% per volume (Putnam, S. A., et at. *J. Appl. Phys.* **2006**, **99**, 084308; Liu, M.-S. L., et al. *Int. J. Heat Mass Transfer*. **2006**, *49*; Patel, H. E., et al. *Appl. Phys. Lett.* **2003**, *83*, 2931−2933). The purpose of this paper is to evaluate the effect of the particle size, concentration, stabilization method and particle clustering on the thermal conductivity of gold nanofluids. We synthesized spherical gold nanoparticles of different size (from 2 to 45 nm) and prepared stable gold colloids in the range of volume fraction of 0.00025−1%. The colloids were inspected by UV−visible spectroscopy, transmission electron microscope (TEM) and dynamic light scattering (DLS). The thermal conductivity has been measured by the transient hot-wire method (THW) and the steady state parallel plate method (GAP method). Despite a significant search in parameter space no significant anomalous enhancement of thermal conductivity was observed. The highest enhancement in thermal conductivity is 1.4% for 40 nm sized gold particles stabilized by EGMUDE (triethyleneglycolmono-11-mercaptoundecylether) and suspended in water with a particle-concentration of 0.11 vol%.

Introduction

Cooling poses one of the major technical challenges facing many industrial sectors such as transportation, microelectronics, and power generation. The common trend to address this problem is to enlarge surface of the heat sink by, for example, incorporating micro-channels into the heat transfer structure.[4−6] However, the performance of such systems could be further increased if one could engineer novel fluids, which provide superior thermophysical properties to conventional fluids. Metals and metal oxides have much higher thermal conductivity than common fluids. Therefore, an innovative way to elevate the thermal conductivity of fluids is the addition of nanometer-sized metal or metal oxide particles into a base fluid. The use of nanometer-sized particles with large specific surface area could not only improve the heat transfer but also provides higher stabilization against particle sedimentation and prevent clogging of the heat sink. Various types of nanoparticles such as metallic [1−3,7,8] and nonmetallic,[9−14] with different shapes and sizes, can be suspended in different fluids forming so-called nanofluids.

A number of the experimental studies on thermal properties of nanofluids show very large enhancements in the thermal conductivity of nanofluids. The most extreme results were obtained for different allotropes of carbon. For example, enormous enhancements of thermal conductivity by 160% and by 70% were observed for a suspension containing 1% of MWCNTs in oil[13] and for 1% ultradispersed diamond in ethylene glycol respectively.[14] Nevertheless those materials are not very stable even at moderate concentrations and need to be studied more carefully in different media.

A variety of oxide particle suspensions were also investigated.[9−14] Due to the moderate thermal conductivity of solid oxides they require high volume fractions (> 5%) to achieve significant thermal conductivity enhancements. The high particle concentrations implicate problems of increased viscosity and colloidal instability which make those suspensions inapplicable for convective heat transfer.

In some cases aqueous nanofluids at vanishing concentrations of "naked" metallic particles such as 50−100 nm copper at 0.001 volume fraction[2] and 10−20 nm gold at 0.00026 vol%[3] were reported to yield thermal conductivity enhancements by up to 23.8% and 21% (at 60 °C) respectively. On the other hand, several other studies demonstrated just moderate, expected enhancements of thermal conductivity for similar fluids. S. A. Putnam et al.[1]

*Corresponding author

(1) Putnam, S. A.; Cahill, D. G.; Braun, P. V.; Ge, Z.; Shimmin, R. G. *J. Appl. Phys.* **2006**, *99*, 084308.
(2) Liu, M.-S. L., Mark Ching-Cheng; Tsai, C. Y. ; Wang, C.-C. *Int. J. Heat Mass Transf.* **2006**, *49*.
(3) Patel, H. E.; Das, S. K.; Sundararajan, T.; Nair, A. S.; George, B.; Pradeep, T. *Appl. Phys. Lett.* **2003**, *83*, 2931–2933.
(4) Escher, W.; Michel, B.; Poulikakos, D. *Int. J. Heat Mass Transf.* **2009**, Under Review.
(5) Escher, W.; Michel, B.; Poulikakos, D. *Int. J. Heat Mass Transf.* **2009**, *52*, 1421–1430.
(6) Tuckerman, D. B.; Pease, R. F. W. *IEEE Trans. Electron Devices* **1981**, *28*, 1230–1231.
(7) Hong, T.-K.; Yang, H.-S.; Choi, C. J. *J. Appl. Phys.* **2005**, *97*, 064311–4.
(8) Assael, M.; Metaxa, I.; Kakosimos, K.; Constantinou, D. *Int. J. Thermophys.* **2006**, *27*, 999–1017.
(9) Li, C. H.; Peterson, G. P. *J. Appl. Phys.* **2006**, *99*, 084314.
(10) Hwang, Y. J.; Ahn, Y. C.; Shin, H. S.; Lee, C. G.; Kim, G. T.; Park, H. S.; Lee, J. K. *Curr. Appl. Phys.* **2006**, *6*, 1068.
(11) Zhu, H. T.; Zhang, C. Y.; Tang, Y. M.; Wang, J. X. *J. Phys. Chem. C* **2007**, *111*, 1646–1650.
(12) Lee, D. *Langmuir* **2007**, *23*, 6011–6018.
(13) Choi, S. U. S.; Zhang, Z. G.; Yu, W.; Lockwood, F. E.; Grulke, E. A. *Appl. Phys. Lett.* **2001**, *79*, 2252–2254.
(14) Kang, H. U.; Kim, S. H.; Oh, J. M. *Exp. Heat Transf.* **2006**, *19*, 181–191.

showed that the enhancement of thermal conductivity was only 1.3% for 4 nm Au particles suspended at 0.35 vol% in ethanol. The contradictory experimental data, reporting anomalous thermal conductivity enhancements could be attributed to poor consideration of particle morphology, size distribution, colloidal stability, or systematic errors in measuring the fluids thermal conductivity.

In this paper a systematic effort was made to produce and to characterize aqueous gold nanofluids. We varied the particle size, the particle loading, and the stabilization method. The gold colloids were characterized by UV−visible spectroscopy, TEM and DLS in order to determine the particle size, morphology and the stability of the colloid. The thermal conductivity measurements were carried out using two independent techniques, namely the transient hot-wire method and the static heated plate method, to eliminate any systematic errors due to the measurement method itself.

Experimental Section

I. Preparation of Gold Nanofluids in the Particle Size Range of 2−40 nm. *Materials*. Hydrogen tetrachloroaurate (III) solution (4.36 M) and silica stabilized gold nanoparticles were supplied by Metalor Technologies SA, Neuchâtel, Switzerland. Trisodium citrate dihydrate (99%), *N*-acetyl-L-cysteine (99%), L-glutathione reduced (98%), tetramethylammonium hydroxide (0.1 M in water), triethyleneglycolmono-11-mercaptoundecylether (95%) (EGMUDE), and aqueous solution of thiol stabilized gold nanoparticles (3−5 nm of diameter, 0.1 vol%) were purchased from Sigma-Aldrich. Ethanol (99.9%) was purchased from Merck. Methanol (99.9%) and sodium borohydride (99%) were purchased from Acros. Glacial acetic acid was purchased from Carlo ERBa. All reagents were used as received. Milli-Q (Millipore) water with a resistivity of 18.2 MΩ was employed throughout. Dialysis membranes (3.5 kDa, Spectra/Por CE) and filtration membranes (0.2 μm, PTFE) were obtained from Spectrum and from Sigma-Aldrich, respectively.

Instrumentation. UV−visible spectra (200−900 nm) were recorded on a Cary 300 spectrometer using a quartz cell of 1 cm path length.

Transmission electron micrographs (TEM) were obtained with a Philips C 200 microscope in bright field mode at a voltage of 200 kV. The samples for TEM study were prepared by casting a few drops of the gold colloid onto carbon-coated copper grids (300 mesh) and used after solvent evaporation in air.

Dynamic light scattering (DLS) was performed with an ALV-5000 spectrophotometer equipped with an argon-ion laser (Coherent Innova 308, λ = 632.8 nm), a digital autocorrelator (ALV) and variable angle detection system. Measurements were made at a fixed scattering angle of 90° and a temperature of 25.0 ± 0.1 °C. The individual correlation functions were analyzed using a second-order cumulate fit. The DLS data were also analyzed with the CONTIN method to obtain the inverse Laplace transformation of the autocorrelation function and the distribution of decay times Γ. The CONTIN data were converted into intensity weighted distributions of hydrodynamic radius.

Preparation of Gold Particles. 1. Gold Colloids with the Particle Size in the Range of 1−3 nm. Spherical gold nanoparticles with diameter of 1−3 nm were prepared using the Brust technique in a single-phase system[15] where an Au(III) chloride salt was mixed with a thiol RSH in a suitable solvent, and subsequently reduced with sodium borohydride $NaBH_4$. Before the reduction step, the thiols were oxidized by gold(III) ions forming Au(I)-SR polymers (see Figure 1):[16,17]

The $HAuCl_4$:RSH molar ratio which controls the average core size was equal to 1:4 for the two syntheses described next.

Synthesis of Glutathione Protected Gold Nanoparticles (*Au_2 nm-SG*). Glutathione (GSH) protected gold NPs were prepared following a previous report.[18] 0.25 mmol of $HAuCl_4$ was added to 50 mL of methanol followed by 1 mmol of glutathione. The solution was cooled in an ice bath for 20 min. We dissolved 2.5 mmol of $NaBH_4$ in 12.5 mL of water that was preliminary cooled to 0 °C and then it was injected rapidly into methanol solution under vigorous stirring. After, the mixture was allowed to react for 90 min in the ice bath. The resulting precipitate was filtered using 0.2 μm PTFE membrane and washed with methanol to remove impurities. The collected precipitate was dissolved in water and the solvent was removed under vacuum at ≤40 °C. The cleaning procedure was repeated several times. Finally, glutathione stabilized gold particles were dialyzed in water during 5 days with replacing water every 10 h. The dialyzed solution was finally evaporated under vacuum resulting in a black powder.

Synthesis of N-Acetyl-L-Cysteine Protected Gold Nanoparticles (*Au_2 nm-NAC*). Gold nanoparticles stabilized by *N*-acetyl-L-cysteine (NAC) were prepared by a procedure described by *Gautier et al.*[19] One mmol (163 mg) of *N*-acetyl-L-cysteine and 0.25 mmol of $HAuCl_4$ were dissolved in 50 mL of 6:1 methanol: acetic acid mixture giving a cloudy white suspension. This is attributed to the formation of Au(I)-NAC polymer. Acetic acid was used to prevent the deprotonation of thiol. 17.5 mL of cold freshly prepared aqueous $NaBH_4$ solution (10 mmol) was carefully added to the Au(I)-NAC polymer solution under vigorous stirring. The black suspension was fast formed and stirred for another 90 min. The precipitate was filtered through the 0.2 μm PTFE membrane, washed with ethanol, dissolved in water and dried under vacuum at $T \leq 40$ °C. After a series of precipitation—filtration (with ethanol) cycles the complete purification of the product was accomplished by dialysis in water over the course of 5 days. The water was changed every 10 h. Final gold colloid was evaporated under vacuum giving a black powder.

The gold colloids with volume fractions up to 1 vol% can be easily prepared through the addition of the powder to a solvent and ultrasonic treatment for 15 min. The resulting solutions are also stable with some content of organic solvent (≤25 vol%) such as methanol, isopropanol, propylene glycol, and stay homogeneous after two hours of heating (≤80 °C).

2. Gold Colloids with Nanoparticles Larger than 16 nm in Diameter. Synthesis of Citrate Stabilized Gold Nanoparticles. The data for the syntheses of gold colloids with the 16−40 nm gold particles are presented in the Table 1.

Spherical gold nanoparticles from 16 to 40 nm in diameter were prepared by citrate reduction of Au(III) as described by Turkevich and Frens.[20,21] In this method, a small amount of $HAuCl_4$ (x mmol) was dissolved in 50 mL of water and heated to the boiling. 1.25 mL of sodium citrate solution with y mmol of the reductant was rapidly introduced into boiling gold solution under continuous heating and vigorous stirring. A color change from pale yellow over colorless to red-wine (or more violet) took place within 15 s. The mixture was kept boiling for 15 min and then cooled to room temperature. The reaction is quite fast, thus the particle size as well as polydispersity depend on many synthesis conditions such as the Au:citrate molar ratio, the concentrations of precursors, the rate of addition of precursors or the temperature of reaction mixture. In our case, the monodispersed gold nanoparticles with different size were synthesized by changing the

(15) Brust, M.; Fink, J.; Bethell, D.; Schiffrin, D. J.; Kiely, C. *J. Chem. Soc., Chem. Commun*. **1995**, 1655.
(16) Negishi, Y.; Takasugi, Y.; Sato, S.; Yao, H.; Kimura, K.; Tsukuda, T. *J. Phys. Chem. B* **2006**, *110*, 12218–12221.
(17) Corbierre, M. K.; Lennox, R. B. *Chem. Mater*. **2005**, *17*, 5691–5696.
(18) Negishi, Y.; Takasugi, Y.; Sato, S.; Yao, H.; Kimura, K.; Tsukuda, T. *J. Am. Chem. Soc*. **2004**, *126*, 6518–6519.
(19) Gautier, C.; Burgi, T. *Chem. Commun*. **2005**, 5393–5.
(20) Frens, G. *Nature, Phys. Sci*. **1973**, *241*, 20–22.
(21) Enustun, B. V.; Turkevich, J. *J. Am. Chem. Soc*. **1963**, *85*, 3317–3328.

Table 1. Synthesis Conditions for Gold Colloids

sample	x ($HAuCl_4$), mmol	y (citrate), mmol	Au:thiol molar ratio	C_M (Au), mM
Au17-cit	0.028	0.084		0.55
Au17-cit	0.0125	0.0375		0.25
Au40-cit	0.0125	0.0221		0.25
Au17-SG[a]			1:5	0.11
Au17-EGMUDE[b]			1:2.5	0.55
Au17-EGMUDE			1:2.5	0.55
Au40-EGMUDE[b]			1:2.5	0.82
Au40-EGMUDE			1:2.5	0.89

[a] Ligand exchange at pH∼9 through an addition of the tetramethylammonium hydroxide (TMeAOH). [b] Ligand exchange via reversible formation of gold nanoparticle-EGMUDE composite assemblies.

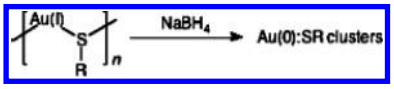

Figure 1. Schematic of synthesis of Au:SR nanoparticles by chemical reduction of Au(I)-SR polymers with $NaBH_4$.

Au:citrate molar ratio and the concentration of precursors (see Table 1).

Surface Modification of Gold Nanoparticles and Preparation of Concentrated Gold Colloids. Gold colloids were purified before ligand exchange generally via dialysis. For this, 50 mL of citrate stabilized gold colloid was placed in a 3.5 kDa membrane and dialyzed against water which was changed every 10 h during a week. In several cases (Au_40 nm-EGMUDE) an ultra filtration technique was used to purify and concentrate the gold colloid. UV−visible spectra analysis and the pH control of gold colloid were used to determine the end of colloid purification by dialysis or by ultra filtration.

Two hydrophilic stabilizers glutathione and triethyleneglycol-11-mercaptoundecylether (EGMUDE) were used to modify the surface of 17 nm gold nanoparticles via reactive thiol groups. The 40 nm gold nanoparticles were covered by EGMUDE.

Typically, the modification of the gold particle surface was carried out by an addition of aqueous solution of ligand to citrate stabilized gold colloid in a respective Au:thiol molar ratio (see Table 1). The resulting colloid was vigorously stirred for 2 h and then kept for several days for the complete ligand exchange. The modified colloid concentrated by rotary evaporation under vacuum at $T \leq 40$ °C giving concentrated gold solution or black powder. Concentrated gold colloids were purified via dialysis against water (see above) while the powders were repeatedly washed with a small quantity of ethanol to remove the excess of thiol and redispersed in a small volume of water or of water−alcohol mixture.

The EGMUDE capped gold colloids (marked by *b*) with a different particle size were prepared otherwise, i.e., via reversible formation of gold-surfactant composite assemblies that was described in a previous report.[22] Briefly, a colloidal (micellar) solution of EGMUDE in water (0.07 mmol in 5 mL) was added to the dialyzed gold colloid (50 mL, 0.55 mM) under stirring. The color of the mixture quickly turned to black and a complete particle precipitation took place within 15 min. After few days without stirring, the gold nanoparticles were successfully self-redispersed forming a homogeneous colloid. The solvent was removed under vacuum at $T \leq 40$ °C. The gold nanoparticles were washed with ethanol and redispersed in water.

(22) Shalkevich, N.; Shalkevich, A.; Si-Ahmed, L.; Bürgi, T. *Phys. Chem. Chem. Phys.* **2009;** DOI: 10.1039B912571J.

II. Thermal Conductivity Measurements. We utilized different techniques to measure the thermal conductivity of electrical conducting liquids. We implemented a static heated plate and a transient hot wire method to eliminate any systematic errors due to the measuring method itself. Additionally, the static heated plate setup requires a smaller fluid volume, which is advantageous for a fast screening of different nanofluid parameters.

The transient hot wire method typically employs a metal wire, immersed into a liquid. The liquid and the metal wire are initially in thermal equilibrium. The wire is exposed to a step voltage resulting in a constant heat generation along the wire. The transient rise in the wire temperature depends on the thermal conductivity of the surrounding liquid whereas the wire temperature is typically measured by the change of electrical resistance. The wire away from its ends behaves like an infinite line heat source surrounded by an infinite volume of liquid. The thermal conductivity of the fluid, λ, can be determined by

$$\lambda = \frac{\dot{q}'}{4\pi(T_2 - T_1)} \ln\left(\frac{t_2}{t_1}\right) \quad (1)$$

where $\dot{q}'$ is the heat generation per unit length and T_2 and T_1 are the absolute temperatures at the time t_2 and t_1 respectively.

The present transient hot wire cell was adapted from the design being proposed by Assael et al. in a series of papers[23−25] (see Figure 2a). A 25 μm thick tantalum wire was used as the heating and sensing wire. We used 500 μm thick tantalum wires as supporting leads to keep the wire in tension and as electrical connections. The wires were electrically insulated from the test fluid by in situ anodization whereby a Tantalum pentoxide layer of about 70 nm was formed at the surface of the wires. A positive bias was applied between the Tantalum wires and the fluid vessel to stabilize the insulating oxide layer. This arrangement also provided the means to observe the leakage current between the wire and the fluid vessel and hence to observe any changes in the quality of the oxide layer.

We used a two wire approach in order to automatically compensate for axial heat conduction at the wire ends. The resistance change of a 20 mm long wire was subtracted from the resistance change of a longer wire being 50 mm in length. This was achieved by connecting each wire to one arm of a Wheatstone bridge. Thus, effectively the resistance change of a 30 mm long segment of an infinite long wire was measured. We directly calibrated the temperature dependence of the resistance of the 30 mm long segment and found a coefficient of 0.0031 K^{-1}, being close to tabulated data for tantalum (0.0036 K^{-1}).

The fluid vessel was made of stainless steel with an inner diameter of 15 mm and a length of 90 mm. The dimensions of the fluid vessel were verified by numerical simulation to ensure that the fluid vessel did not influence the transient temperature response of the sensing tantalum wire. The total required fluid volume for one measurement amounts to 18 mL. To control the fluid temperature, the fluid vessel was surrounded by a water jacket.

We measured the wire resistance before heating by applying an input current of 3 mA. Afterward, the wire was heated in a constant voltage mode, whereas the voltage was adapted to the fluid properties to produce temperature rises between 3 and 4 K in a measurement period of 1.5 s. The transient temperature rise of the wire was measured at a sampling rate of 500 Hz by a digital multimeter. We performed 10 iterations to determine thermal conductivity of a sample within a standard deviation of less than 0.5%. The absolute maximum error was determined by thermal

(23) Assael, M. J.; Karagiannidis, L.; Malamataris, N.; Wakeham, W. A. *Int. J. Thermophys.* **1998**, *19*, 379–389.
(24) Assael, M. J.; Chen, C. F.; Metaxa, I.; Wakeham, W. A. *Int. J. Thermophys.* **2004**, *25*, 971–985.
(25) Assael, M. J.; Charitidou, E.; Georgiadis, G. P.; Wakeham, W. A. *Berichte Bunsenges. Phys. Chem.* **1988**, *92*, 627–631.

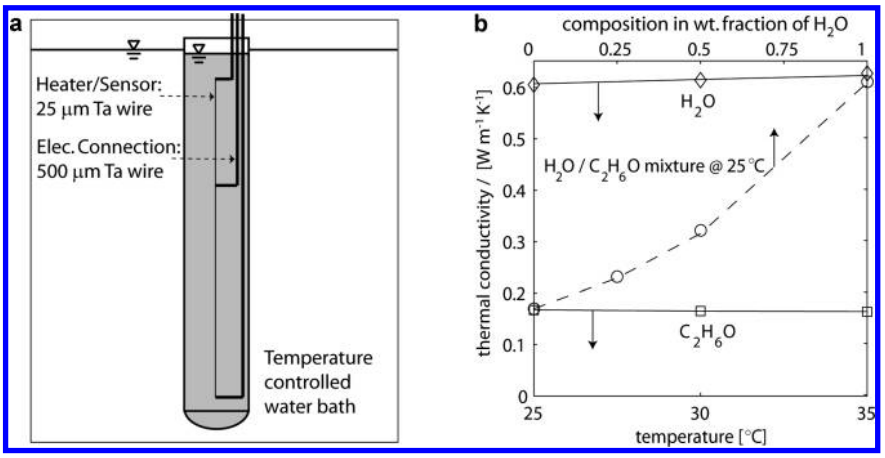

Figure 2. (a) Schematic of transient hot wire cell, (b) thermal conductivity of ethanol and water at different temperatures and thermal conductivity of water/ethanol mixtures at different concentrations measured with present transient hot wire cell, markers indicate the measured values and lines reference data from literature (H_20 and C_2H_6O data extracted from NIST Standard Reference Tables, data for fluid mixtures extrapolated from Assael et al.[25]).

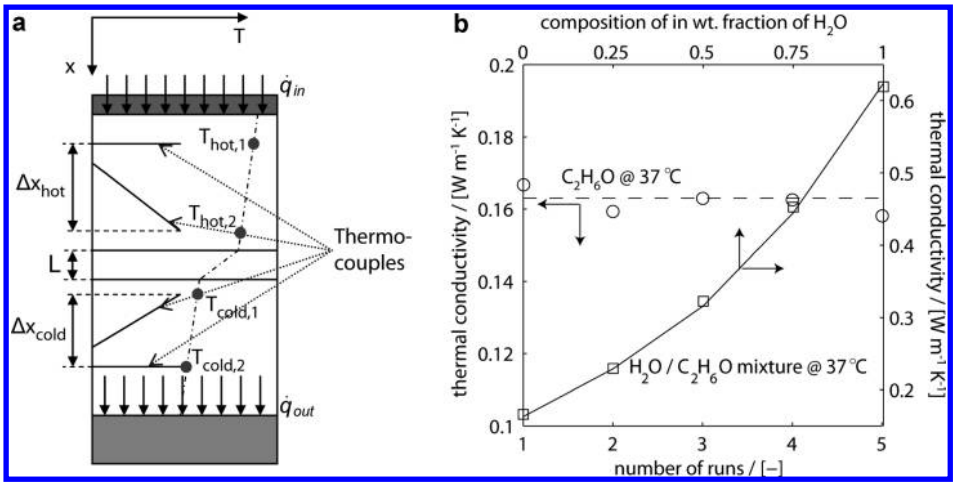

Figure 3. (a) Schematic static heated plate set up − (b) thermal conductivity of ethanol and of water/ethanol mixtures at different concentrations measured with present static heated plate method at 37 °C, markers indicate the measured values and lines reference data from literature (C_2H_6O data extracted from NIST Standard Reference Tables, data for fluid mixtures interpolated from Assael et al.[25]).

conductivity measurements of water, water/ethanol mixtures, and ethanol in a temperature range of 298−323 K and is specified to be less than 2.5% (see Figure 2b).

The static heated plate method is based on Fourier's law of heat conduction. We generate a one-dimensional heat flux across a thin fluid layer. If the temperature difference across the fluid layer, ΔT, the thickness of the fluid layer, L, and the heat flux per unit area, $\dot{q}''$ are known, we can compute the thermal conductivity of the fluid from,

$$\lambda = \frac{\dot{q}'' L}{\Delta T} \tag{2}$$

A schematic of the static heated plate methods is shown in Figure 3a. The heating was provided by a thin film heater called "Cobra" deposited on the back of a 21 × 21 × 1 mm^3 silicon die. Three temperature sensors were deposited at the same time. The heat flowed downward through a 20 mm diameter, 20 mm long copper piece where two 0.5 mm diameter K-type thermocouples had been embedded. At the end of the copper part, the heat flowed through the liquid layer into a second copper piece, similar to the first one. A Mikros cooler connected to a chiller functioned as heat sink. A glass-ceramic (Macor) cylinder provided at the same time thermal insulation for the copper pieces and containment for the liquid enclosed between the two copper slugs and the glass-ceramic. Two o-rings provided the required sealing around the copper parts.

The liquid was introduced through a capillary tube glued to the Macor part. A second tube functioned as drain for the trapped air. The minimum fluid volume for one measurement was determined to be 2 mL.

The gap between the two copper pieces was measured by four linear variable differential transformer calipers and could be adjusted with 4 screws. In our experiments we chose gab dimensions between 200 and 300 μm. Natural convection was suppressed as the heat flowed from the top to the bottom and an bull's eye level was used to ensure that the set up was kept in a horizontal position. In any event, the Rayleigh number of the present apparatus was always kept much smaller than the critical value of 1700.

During a measurement, a constant heat flux of about 20−30 W was applied and the temperature profiles in both copper slugs were measured. Assuming a linear temperature profile within the copper cylinders, the temperatures at the solid fluid interface could be interpolated. Hence, if steady state conditions were established, the thermal conductivity of the fluid could be calculated according to eq 2.

Due to thermal expansion of the system, the exact gap between the copper cylinders could not be determined by the calipers, hence, we used this distance as a calibration factor and corrected

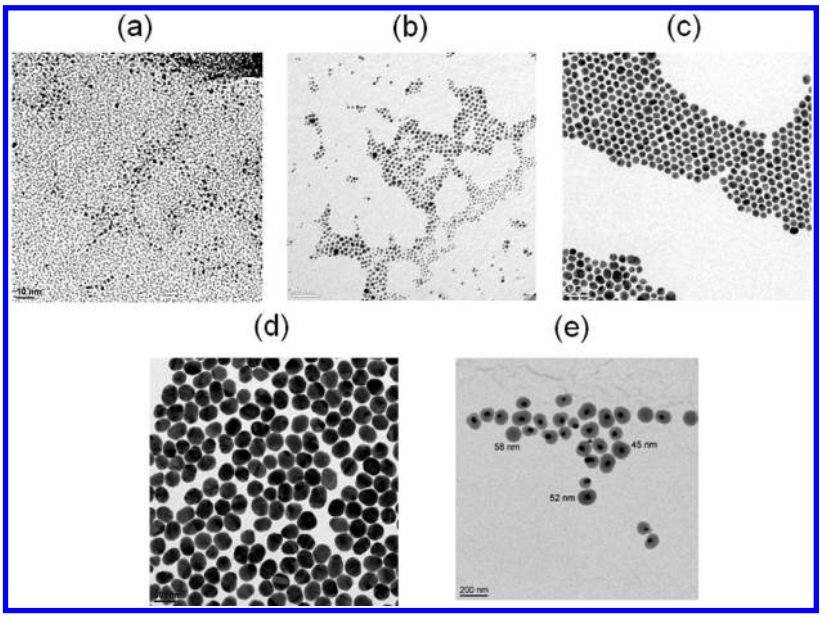

Figure 4. Transmission electron microscopy graphs of gold nanoparticles of different size: (a) Au-SG nanoparticles with an average diameter of 2 nm, Au-EGMUDE nanoparticles with diameter of 4 nm (b), of 17 nm (c), of 40 nm (d) and Au-silica nanoparticles with a 45 nm in gold core.

for the distance to match the thermal conductivity of water. The error of the method was determined by test measurements with water/ethanol mixtures and ethanol and was identified to be less than 3% (see Figure 3b).

Results and Discussion

Preparation of Gold Nanofluids. Spherical gold nanoparticles of sizes from 2 to 40 nm were synthesized in water or water−alcohol mixture by reduction of gold(III) salt. The particle size has been controlled by varying the reducing agent (and/or stabilizer)/gold ratio. Typical TEM micrographs of gold nanoparticles with different sizes are shown in Figure 4.

The gold particles of 2 nm (Figure 4a) have been produced in powder form. The nanopowders have been extremely stable and did not show any signs of decomposition, such as loss of solubility or particle growth, even in a year of storage at ambient temperature in air. The powder was dispersed in water or water−methanol mixture giving homogeneous concentrated colloids. This way allows us to obtain extraordinary concentrated stable gold colloids with volume fraction up to 1 vol%. The stability of highly concentrated colloids with small gold nanoparticles can be attributed to combined charge and steric protection provided by hydrophilic GSH or NAC layers on the gold surface.

The gold nanoparticles with diameter more than 16 nm (Figure 4c and d) were synthesized by citrate reduction forming the stable Au-citrate colloids at volume fraction less than 0.00055 vol%. Concentrated colloids of the Au−citrate nanoparticles cannot be directly achieved, because of agglomeration and precipitation due to insufficient protection of gold surface by citrate ions. In order to produce more concentrated nanofluids with large and heavy gold particles the steric stabilization of gold surface is most importantly required. Several hydrophilic stabilizers with thiol headgroup and a hydrophilic part were used to modify the surface of gold-citrate nanoparticles and enhance nanoparticle stability. Ligand exchange with GSH and EGMUDE resulted in concentrated 17 nm gold colloids at 0.0036 and 0.33 vol%, respectively. Both concentrated gold colloids contained small amounts of the precipitate that could be due to incomplete replacing of citrate by GSH and EGMUDE.

The highly concentrated colloids of 17 and 40 nm gold nanoparticles stabilized with EGMUDE were successfully produced by the method of reversible formation of gold-surfactant composite assemblies described in detail elsewhere.[22] This method directly gives very stable particles at high concentration (up to 0.4 vol%). Efficient surface coverage results in concentrated suspension which remain stable even at high temperature (up to 70 °C).

Thermal Properties of Gold Nanofluids. Experimental data for the relative thermal conductivity of different gold nanofluids are summarized in the Table 2. Water and methanol−water mixture were used to prepare the nanofluids which could be utilized as coolants for microelectronic devices. Water was chosen because of its excellent thermophysical properties, i.e., low viscosity, very high specific heat, and high thermal conductivity. However, the high freezing point and the thermal expansion under freezing confine the temperature work range of water in closed systems. Addition of methanol up to 24% decreases the freezing point of water to −19.1 °C[26] but simultaneously reduces the heat transfer capacity and increases the viscosity of fluid. Nevertheless, methanol seems a suitable water-miscible solvent to decrease the freezing point of water.

For each sample, the thermal conductivity of the reference fluid was measured independently at the same temperature as the gold nanofluid. The temperature of measurement was varied between 25 and 40 °C. Stabilizer was added in the reference fluid (water or water−methanol mixture) to consider its influence on the thermal conductivity of the suspension. The stabilizer amount was taken equal to the quantity of stabilizer adsorbed on the gold particle surface.

The gold nanoparticles were stabilized in different ways. The gold-citrate nanoparticles have charge stabilization due to physically absorbed citrate ions on the gold surface. Such nanoparticles, usually named as "naked" particles, form stable nanofluids only at volume fractions less than 0.001 vol%. Therefore, the stable concentrated colloids require a replacement of citrate by a

(26) Lide, D. R., *CRC Handbook of Chemistry and Physics*, 89th ed; CRC Press: Boca Raton, FL, 2008.

Table 2. Thermal Conductivity of Gold Colloids

particle size, nm	stabilizer	base fluid	particle volume fraction, %	relative thermal conductivity	method of measurement
2	NAC	methanol/water	0.1	0.996 (39 °C)	GAP
			0.2	0.990 (39 °C)	GAP
			1	0.952 (39 °C)	GAP
	GSH	methanol/water	0.1	1.01 (39 °C)	GAP
			0.2	0.989 (39 °C)	GAP
			1	0.959 (39 °C)	GAP
4	EGMUDE	water	0.1	0.997 (37 °C)	GAP
17	citrate	water	0.00025	1.013 (25 °C)	THW
			0.00025	0.997 (40 °C)	THW
			0.00025	1.004 (39 °C)	GAP
			0.00055	1.015 (25 °C)	THW
			0.00055	1.01 (40 °C)	THW
	GSH	water	0.0036	0.998 (33 °C)	GAP
	EGMUDE[b]	methanol/water	0.008	0.977 (25 °C)	THW
	EGMUDE[b]	methanol/water	0.018	0.972 (25 °C)	GAP
	EGMUDE[b]	methanol/water	0.07	0.992 (25 °C)	GAP
	EGMUDE	water	0.33	1.013 (25 °C)	GAP
40	EGMUDE[b]	water	0.078	1.006 (37 °C)	GAP
	EGMUDE	water	0.11	1.014 (37 °C)	GAP
45	Silica	water	0.4	1.002 (25 °C)	THW

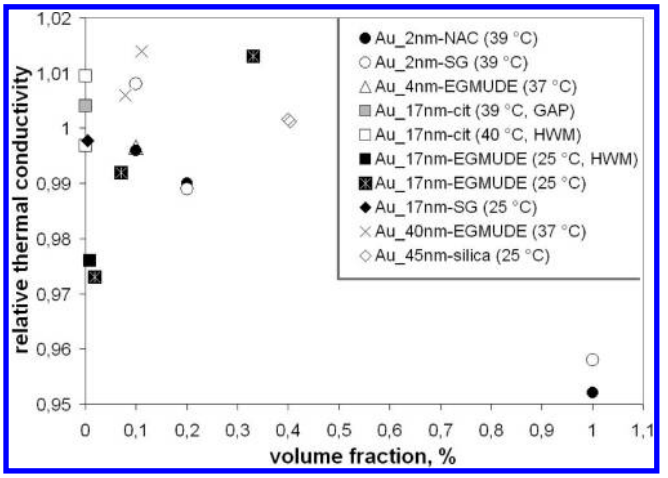

Figure 5. Relative thermal conductivity of gold nanofluids as a function of volume fraction.

more sufficient stabilizer. The surface modification was performed by chemical covering (with thiols and silica) of gold particles in order to improve particle stability and to gain highly concentrated gold colloids.

The gold nanofluids in the particle (core) size range from 2 to 45 nm and at volume fraction from 0.00025 to 1 vol% were prepared and tested.

Figure 5 shows the effect of volume fraction on relative thermal conductivity of gold colloids. Most of the nanofluids were tested by the GAP method as it requires less fluid volume. Commonly, the tendency of thermal conductivity enhancement with increase of nanoparticle concentration is observed. However, the tested fluids showed only small changes of thermal conductivity being within the range of the measurement uncertainty. The nanofluids consisting of the Au-EGMUDE particles with diameter of 17 or 40 nm have a small thermal conductivity enhancement at volume fraction larger than 0.07 vol%. The highest gain of thermal conductivity was observed for Au_40 nm-EGMUDE colloid with 0.11 vol%. Several gold nanofluids were tested by both the GAP and the THW methods and no appreciable difference between thermal conductivity values for the same nanofluid measured with the two methods was observed.

Table 3. Stabilizer Content in Covered Gold Nanoparticles

diameter, nm	kind of stabilizer	Au/stab molar ratio	Au/stab volume ratio
2	GSH	6.7	0.165
2	NAC		0.315
2	EGMUDE	5.94	0.019
4	EGMUDE	11.9	0.08
17	EGMUDE	50.5	0.755
40	EGMUDE	118.9	2.11

Surprisingly, the smallest nanoparticles with diameter of 2 nm exhibit even an inverse tendency and thermal conductivity decreasing with increasing of volume fraction. Thus, the nanofluids of Au_2 nm-SG and of Au_2 nm-NAC particles at maximum concentrations (1 vol%) have the relative thermal conductivities of 0.959 and 0.952, respectively, i.e., thermal conductivity lower than for base-fluids (0.636 W/(m·K) and 0.635 W/(m·K), respectively).

Such "negative" tendency for very small particles can be explained by two factors. The first one is the discrete nature of subnanometer gold particles[27], i.e., the presence of discrete energy levels in the electronic structure of metal nanocrystals. The level pattern near the highest occupied level is critically sensitive to size and shape of the metal crystallite and essential to describing its properties (thermal, chemical, electrochemical).[28] In fact, such small particles are not metallic and that might account partially for lower thermal conductivity of subnanometer particles. Second, the stabilizer layer can act as thermal insulator because of its low thermal conductivity. The stabilizer effect can be assessed through a calculation of Au/stabilizer molar and volume ratio for a spherical gold particle with well-packed monolayer of stabilizer (see Table 3). Here, the length of the individual EGMUDE molecule in fully extended mode was taken as 2.76 nm and the average thickness of NAC and GSH monolayers were assumed as 0.61 and 0.92 nm respectively.

The Au/stabilizer volume ratios are much less than 1 despite reasonably high molar ratio. Therefore, we can treat the 2 nm gold nanoparticles as partially isolated for heat transfer.

(27) Barnett, R. N.; Cleveland, C. L.; Häkkinen, H.; Luedtke, W. D.; Yannouleas, C.; Landman, U. *Eur. Phys. J. D* **1999**, *9*, 95–104.
(28) Schaaff, T. G.; Shafigullin, M. N.; Khoury, J. T.; Vezmar, I.; Whetten, R. L.; Cullen, W. G.; First, P. N.; Gutierrez-Wing, C.; Ascensio, J.; Jose-Yacaman, M. J. *J. Phys. Chem. B* **1997**, *101*, 7885–7891.

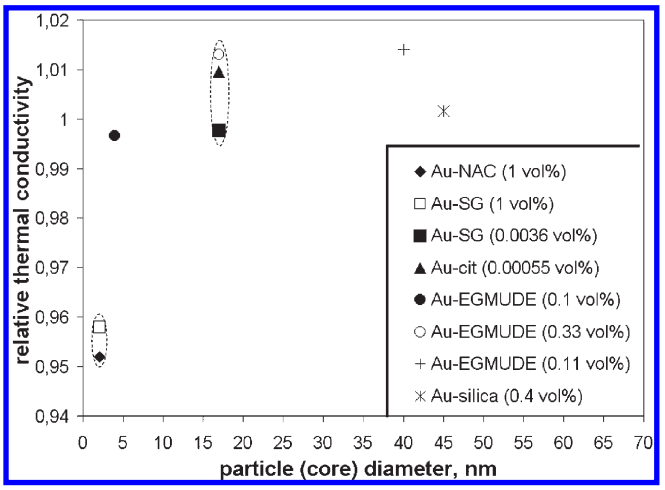

Figure 6. Relative thermal conductivity of gold nanofluids as a function of particle size.

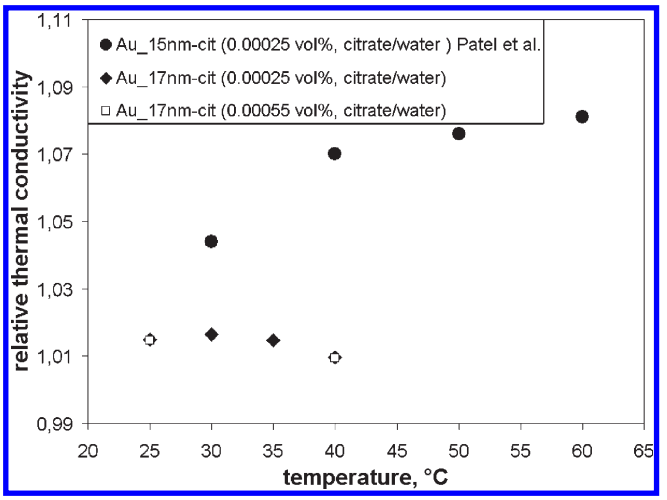

Figure 7. Relative thermal conductivity of gold-citrate nanofluids as a function of temperature.

Figure 6 presents the relative thermal conductivity as a function of particle size. Indeed, there is a clear tendency of decreasing thermal conductivity with decreasing particle size in the range of 2−40 nm. A similar tendency was observed for alumina nanoparticles dispersed in ethylene glycol. Xie et al.[29] reported a doubled enhancement of thermal conductivity for the 60 nm alumina particles as compared to the 15 nm particles. That contradicts to the commonly stated influence of particle size, i.e., the improvement of thermal conductivity due to increased specific surface area of the dispersed phase.[2,3,10,12,14]

The importance of the shell composition to the heat transfer can be illustrated as well by the data for 17 nm particles (see Figure 6). We have tested three kinds of surface modifiers, i.e., the citrate, glutathione (GSH), and EGMUDE. The latter two are chemically bound to the gold surface, whereas the former enables charge stabilization of the gold nanoparticles. The gold-citrate nanofluid at 0.00055 vol% exhibits thermal conductivity enhancement in the same range as nanofluids with EGMUDE modified particles, even though the latter had a 600 times higher concentration. The system with glutathione as a modifier even reveals the same thermal conductivity as basefluid (0.622 W/(m·K)).

The chemical nature of the nanoparticle shell plays an important role for heat transfer. Min Hu et al.[30] demonstrated higher heat dissipation rates for 15 nm silica coated gold nanoparticles, compared to citrate stabilized gold particles even when the silica layer is thicker than 10 nm. Therefore, we prepared and tested 45 nm gold nanoparticles with 40 nm silica coating (see Figure 4e). Unfortunately, no thermal conductivity enhancement was observed for silica stabilized 45 nm gold nanofluid at 0.4 vol%. That could be attributed to the properties of the silica shell which depend on the production and processing of the silica shell. The highest cooling rates should be obtained for shells that are well formed and have thermal properties that are close to fused silica. Porous shells that have a significant solvent penetration will have lower cooling rates.[30]

The citrate stabilized nanofluid agrees in terms of particle material, size and morphology with a previous published study of Patel et al.[3] Furthermore, the colloids are prepared and stabilized by the same procedure. A comparison of the obtained thermal conductivity is summarized in Figure 7.

Our experimental data at two volume fractions (2.5×10^{-6} and 5.5×10^{-6}) shows very similar behavior with quite small thermal conductivity enhancements and without any temperature dependence. Furthermore, we measured the thermal conductivity by means of both measurement techniques. The obtained data is in close agreement, whereby our results are additionally corroborated. Our observations deviate from the data of Patel et al.[3] where significant conductivity enhancement especially at elevated temperatures was reported.[3] A possible reason for such an effect can be colloid destabilization causing particle clustering and/or their sedimentation on the detector surface and significantly change the thermal conductivity measurement in Patel et al. In order to investigate possible destabilization of the colloid under heating we have performed light scattering measurement of naked colloids at different temperatures.

Figure 8a shows the correlation functions for the Au_17 nm-citrate colloids at different temperatures. All correlation curves have the same shape and differ only in lag times. This shift results from decreasing water viscosity and therefore increasing diffusion coefficient of the gold nanoparticles. For all three curves the cumulative analysis provides a hydrodynamic radius of the particles of around 10 nm. Hence, we cannot observe any temperature dependency of the colloid clustering behavior. Absence of any structural change of the nanofluid with 17 nm gold particles is well coherent with our invariant relative thermal conductivity at different temperature.

We also tested the influence of cluster formation on the thermal conductivity. Figure 8b shows particle size distributions of gold colloids of Au_40 nm protected by different stabilizers at 0.12 mM. Citrate capped gold nanoparticles show quite low polydispersity with a mean hydrodynamic radius of 20 nm. After reverse precipitation[22] with EGMUDE protection the mean hydrodynamic radius grew up by 2.5 nm due to the additional layer of stabilizer. The polydispersity is almost the same, contrary to the behavior of particles after classical ligand exchange. There we observe not only much higher polydispersity but also increased mean hydrodynamic radius, which clearly implies relatively small (2−3 particles) clusters even in a well diluted colloid (at 0.12 mM). Those transformations were also confirmed by UV−vis spectroscopy (Figure 8c). The suspensions with citrate capped particles and stabilized by EGMUDE by means of reverse stabilization have almost the same spectra with small red-shift of 3 nm for

(29) Xie, H.; Wang, J.; Xi, T.; Liu, Y.; Ai, F.; Wu, Q. *J. Appl. Phys.* **2002**, *91*, 4568–4572.
(30) Hu, M.; Wang, X.; Hartland, G. V.; Salgueiriño-Maceira, V.; Liz-Marzán, L. M. *Chem. Phys. Lett.* **2003**, 372.

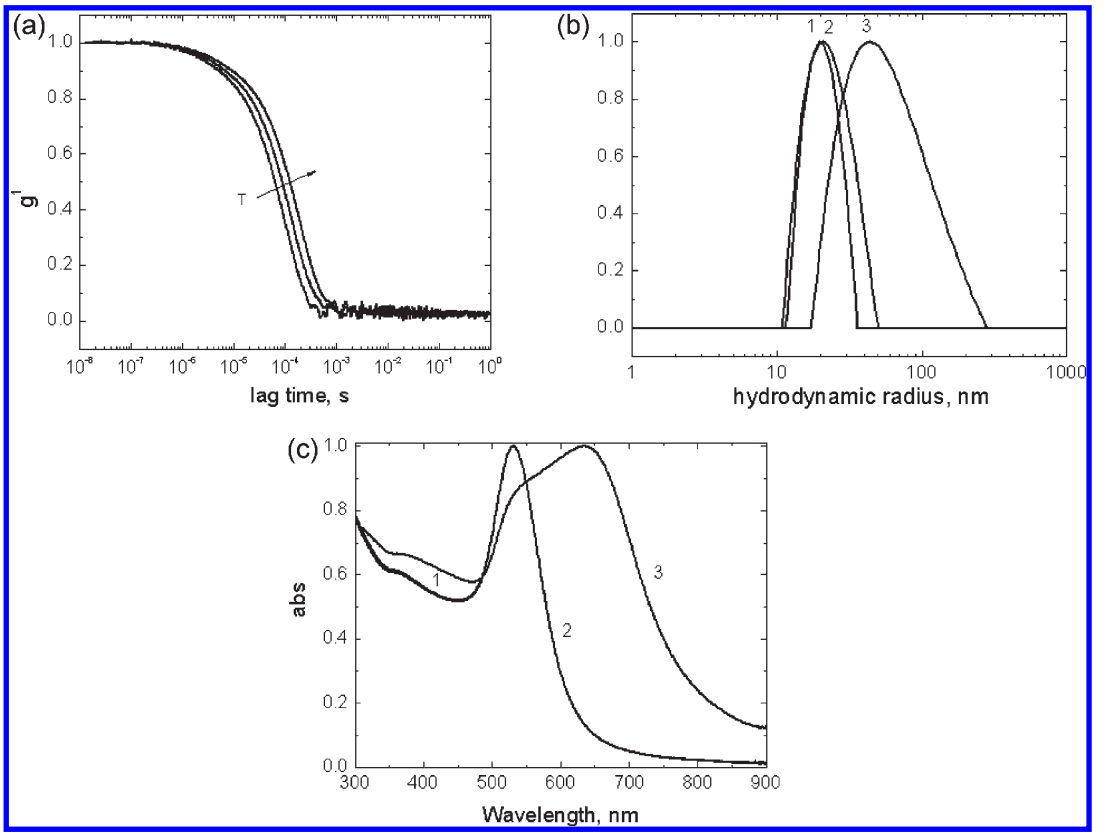

Figure 8. (a) The normalized electric field autocorrelation functions of 17 nm gold colloids at 0.55 mM at different temperatures: 20, 40, and 60 °C. (b) particle size distributions of 40 nm gold colloids at 0.12 mM with different stabilizers: citrate (1), EGMUDE after reverse precipitation (2) and EGMUDE after simple citrate replacement (3). (c) UV−vis normalized spectra of 40 nm gold colloids at 0.12 mM with different stabilizers: citrate (1), EGMUDE after reverse precipitation (2), and EGMUDE after simple citrate replacement (3).

Au-EGMUDE particles. On the other hand the UV−visible spectra of nanoparticles covered with EGMUDE by classical ligand exchange consists of a single particle plasmon band at 531 nm and a secondary surface plasmon band at 635 nm which is associated with formation of aggregates. The position of the latter depends on the interparticle separation (ligand length). According to Sendroiu et al.[31] the spectral aggregation shift becomes more pronounced with decreasing relative distance $d/2R$, where d is separation between particle centers and R is particle radius. For Au_40 nm-EGMUDE colloid prepared by classical ligand exchange the spectral aggregation shift is 635 nm-531 nm = 104 nm that corresponds to $d/2R \leq 1.1$ (see Sendroiu et al.[31]). This means that the interfacial particle distance is much lower than 4 nm (20 nm × 2 × 1.1 − 20 nm × 2 = 4 nm) that is less than double the length of EGMUDE molecule in an elongated state (2 × 2.76 nm = 5.52 nm). This can be related to incomplete citrate substitution by EGMUDE causing the cluster formation. Nevertheless, we do not observe any significant variations of the thermal conductivity for the samples with different particles stability.

Within the context of effective medium theory the largest possible increase of thermal conductivity for nanofluids with spherical particles at volume fraction $\varphi \ll 1$ will be $3\varphi\lambda_0$ (where λ_0 is thermal conductivity of basefluid) resulting in thermal conductivity enhancements $<1.8\%$ for volume fractions $\varphi < 0.01$. Hence, all our data is consistent with effective medium theory.

(31) Sendroiu, I. E.; Mertens, S. F.; Schiffrin, D. J. *PCCP* **2006**, *8*, 1430–6.

Conclusions

In this paper, we produced stable gold colloids for a wide range of particle sizes (2−45 nm) and concentrations (0.00025−1 vol%). The particles are either protected solely by citrate ions or covered by chemically bounded ionic or nonionic stabilizers. We investigated the influence of these parameters as well as the temperature on the thermal conductivity of gold nanofluids by both GAP and THW methods. In spite of the large number of samples at different concentrations we did not observe a significant enhancement in thermal conductivity for any gold nanofluid. We additionally considered the effect of the particle clustering and did not find any dependence at least for small cluster sizes. The largest relative thermal conductivity of 1.014 was observed for the 0.11 vol% Au_40 nm-EGMUDE nanofluid, whereas a similar enhancement was achieved for the Au_17 nm-citrate nanofluid at a low gold concentration of 0.00055 vol%. Consequently we conclude that there is no abnormal thermal conductivity enhancement, i.e., any deviation from classical effective medium theory for low concentrated well-dispersed aqueous gold nanofluids.

Acknowledgment. We thank Andrey Shalkevich for his help with the DLS experiment and fruitful discussions. This work was supported by the Bundesamt für Berufsbildung und Technologie in the frame of a KTI project.